Resource-aware Deployment of Dynamic DNNs over Multi-tiered Interconnected Systems

Resource-aware Deployment of Dynamic DNNs over Multi-tiered Interconnected Systems

C. Singhal[1], Y. Wu[2], F. Malandrino[3,4], M. Levorato[2], C. F. Chiasserini[5,4,6]
1: Indian Institute of Technology Kharagpur, India – 2: UC Irvine, USA – 3: CNR-IEIIT, Italy
4: CNIT, Italy – 5: Politecnico di Torino, Italy – 6: Chalmers University of Technology, Sweden

***Abstract*—The increasing pervasiveness of intelligent mobile applications requires to exploit the full range of resources offered by the mobile-edge-cloud network for the execution of inference tasks. However, due to the heterogeneity of such multi-tiered networks, it is essential to make the applications' demand amenable to the available resources while minimizing energy consumption. Modern dynamic deep neural networks (DNN) achieve this goal by designing multi-branched architectures where *early exits* enable sample-based adaptation of the model depth. In this paper, we tackle the problem of allocating sections of DNNs with early exits to the nodes of the mobile-edge-cloud system. By envisioning a 3-stage graph-modeling approach, we represent the possible options for splitting the DNN and deploying the DNN blocks on the multi-tiered network, embedding both the system constraints and the application requirements in a convenient and efficient way. Our framework – named Feasible Inference Graph (FIN) – can identify the solution that minimizes the overall inference energy consumption while enabling distributed inference over the multi-tiered network with the target quality and latency. Our results, obtained for DNNs with different levels of complexity, show that FIN matches the optimum and yields over 65% energy savings relative to a state-of-the-art technique for cost minimization.**

I. Introduction

Deep Neural Networks (DNN) are a pervasive paradigm that empowers a wide range of applications with advanced data analysis and decision making capabilities. Examples include computer vision [1], speech recognition [2], natural language processing [3], and mobile health care [4]. However, the complexity and energy consumption [5] of modern DNNs clashes with the limited computing power and energy reservoir of mobile platforms and embedded devices.

Two main technical strategies attempt to address this issue: model compression [6] and edge computing [7]. In the former, the size and complexity of large DNN models are reduced using techniques such as pruning, quantization, and knowledge distillation. However, compression often results in a noticeable loss of inference performance, and in many mobile settings the execution of even compressed models necessitates a considerable amount of power. In edge computing, a compute-capable node positioned at the network edge takes over the execution of the DNN. Edge computing suffers from the need to transfer information-rich signals over a volatile wireless channel, often under tight latency constraints. Additionally, in real-world systems, edge servers likely need to support a multitude of applications and users, which may overload their computing and communications capabilities.

Recently, a variant of edge computing emerged where DNN models are divided into *sections* that are distributed over mobile-edge-cloud systems. This approach is often referred to as "split computing" or "split DNN" [8]. *By controlling the splitting points defining the sections of the DNN, one can control the computing load allocated to the different devices/servers as well as the amount of data transmitted on the communication links connecting them.* In fact, each node is tasked with the execution of a portion of the DNN, and is thus in charge of a fraction of the overall operations. Moreover, instead of the input, the *sections transmit their output tensors, whose size is a function of the splitting point*. Relevant work in this direction includes [9]–[13], as discussed in Sec. VI.

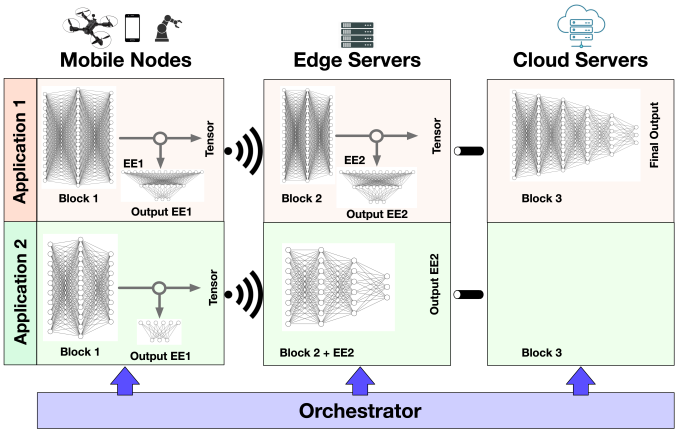

Fig. 1. Our framework allocates blocks of layers of DNNs with early-exits (EEs) to mobile-edge-cloud systems so that energy expenditure is minimized. Multiple applications coexist, and an orchestrator controls the execution of DNN blocks and information flow across them based on application requirements (accuracy and latency) and system constraints (bandwidth, computing capacity). For Application 1, the orchestrator allocates two blocks with early exits (EE1 and EE2) to a mobile node and an edge server, while for Application 2 the target performance is achieved by using the first two early exits.

In this paper, we tackle *the split DNN problem in the context of dynamic DNNs – and, specifically, multi-branched DNNs equipped with early exits [8], [14], [15] – and multi-tiered mobile-edge-cloud systems* (Fig. 1). The motivation behind these architectures is that, to achieve high performance in complex tasks, DNNs have to deal with the most challenging samples in a dataset. This results in models that are over-parametrized for a large set of the input samples. Early exits are model-tails attached to some layers of the original model designed to produce an analogous output as that of the full DNN, with a smaller computing effort. By deciding which branches to execute sample-by-sample, early-exit models can dynamically adapt the number of operations needed to produce an output to the input "complexity". An overview on early-exit DNNs and related challenges can be found in [8], [16].

Our work focuses on the problem of allocating "blocks" of layers of DNNs with early exits to the nodes composing the overall mobile-edge-cloud system. Notably, unlike most of the existing studies on split DNNs, we consider a setting with multiple data sources, applications, and nodes at all the tiers of the infrastructure (see Fig. 1). Also, it is worth remarking that the presence of early exits influences the flow of information throughout the blocks, and some executions may be terminated early, further complicating the allocation problem. The overall allocation problem we formulate minimizes the energy needed to complete inference under latency and accuracy application requirements, as well as bandwidth and computing resource constraints. To resolve this challenging – NP-hard – problem, we adopt an approach based on graph optimization, where we manipulate an initial graph capturing the relationship between system nodes and DNN layers to create a specialized graph which we can be used to compute feasible low-cost paths (corresponding to allocation strategies).

In summary, the contributions of this work are as follows:

1) We formulate an allocation problem where the blocks of DNNs layers with early exits required by mobile applications are allocated to the nodes of a mobile-edge-cloud system. The objective is to minimize energy consumption while satisfying application-specific inference requirements, under computing power and channel capacity constraints.
2) We devise a new solution framework – named Feasible Inference Graph (FIN) – for the allocation problem. By manipulating the graph describing the DNN block allocation problem, we build a graph model amenable to optimization, which only contains paths representing feasible solutions and where the optimal allocation is the minimum-cost path.
3) We explore the impact on the inference energy consumption of different allocation configurations for three DNN models with early exits (B-LeNet, B-AlexNet and B-ResNet, pre-trained on multiple datasets), over nodes with different computing and communication capabilities.
4) Our results show that models equipped with early exits can dramatically decrease the overall energy consumption when some of these exits are allocated to mobile or edge devices under system and application-level constraints, by reducing the involvement of larger-scale nodes in the completion of the inference. We also show how FIN performs close to the optimum computed by brute force. Compared to the state-of-the-art approach in [17] for cost minimization, FIN yields dramatic energy savings, exceeding 90% of the computational energy and 80% of the communication one. Furthermore, such gains are consistent under different branchy DNN architectures, from the small-scale B-LeNet to the much larger B-AlexNet.

II. Energy-aware Inference through Dynamic NNs

First, we introduce the mobile-edge-cloud system, along with the structure of the DNN models and applications. We also describe the corresponding two-plane graph capturing the possible allocation of DNN blocks (Plane 1) to the system nodes (Plane 2), along with the nodes computing and communication resources (Sec. II-A). Then we translate the two-plane graph into a single-plane extended graph (Sec. II-B), used to optimally configure dynamic DNNs for energy-efficient inference tasks (Sec. II-C). We later develop a low complexity solution using this extended graph that gives performance close to optimum.

TABLE I
Notation

Symbol	Definition
$s \in \mathcal{S}$	Data sources
$n \in \mathcal{N}$	Multi-tiered network nodes
$h \in \mathcal{H}$	Applications (or, equivalently, DNN models)
$\widetilde{\mathcal{G}}=\{\widetilde{\mathcal{V}}, \widetilde{\mathcal{E}}\}$	Two-dimensional two-plane graph modeling the overall system
$\mathcal{G}=\{\mathcal{V}, Ec\}$	Single-plane extended graph
ℓ_i^h	i-th block of application h's DNN
σ^h	Inference rate for application h
α^h	Target inference quality of application h
δ^h	Target inference latency of application h
$\phi^h(\ell_i^h)$	Fraction of input samples that are output by ℓ_i^h
$T^h(v,v')$, $C^h(v,v')$, $E^h(v,v')$	Data transfer time, computing time, and energy consumption weights of the edge $v \rightarrow v' \in \mathcal{E}$, with $v=(n,\ell_i^h)$ and $v'=(n',\ell_j^h)$
π^h	Path on $\mathcal{G}$ representing a configuration of application h
γ	Resolution of the feasibility graph

A. System model

We consider a multi-tiered communication and computing infrastructure composed of mobile nodes, edge servers, and cloud servers. The objective of the overall system is to support a set of mobile applications whose central component is a DNN performing the analysis of the information that the mobile nodes acquire through co-located data sources. Examples include computer vision models for object detection and image classification, as well as speech recognition tasks. The edge of the infrastructure hosts a Machine Learning (ML) orchestrator that possesses knowledge of the applications, as well as some essential information about the capabilities of the mobile nodes and the data they can acquire.

Formally, the main elements defining the system are:

- A set $\mathcal{S}$ of data sources (e.g., sensors) indexed with $s \in \{1, \ldots, S\}$; each data source samples a physical phenomenon extracting information that serves as input to an inference task for application h at rate $\sigma^h \geq 0$.
- A set $\mathcal{N}$ of computationally-capable network nodes, including (i) mobile nodes connected to data sources, (ii) edge servers, and (iii) cloud servers.
- A set $\mathcal{H}$ of applications $h \in \{1, \ldots, H\}$, each associated with a DNN model equipped with early-exits. We describe the overall architecture of the DNN associated with application h as composed of a set of layer blocks $\mathcal{L}^h = \{\ell_1^h, \ldots, \ell_N^h\}$, where *each block corresponds to a portion of the network backbone and at most one early exit*. Although the input

rate of the application is σ^h, early exits may "capture" some input and terminate execution; we thus define $\phi^h(\ell_i^h)$ as the fraction of input samples that are output after block ℓ_i^h. Each application h has specific requirements defined as the target inference quality (e.g., target accuracy value) α^h, and maximum inference latency δ^h. In the following, we often refer to applications and the DNN representing their essential component interchangeably.

Given application h, the ML orchestrator determines which blocks of the DNN should be executed and assigns them to network nodes in such a way that the application inference requirements are fulfilled. Specifically, according to the split computing paradigm, the network nodes can cooperatively execute the overall DNN: a node assigned a DNN block or a set of blocks will execute all the corresponding layers and send the output coefficients of their cut layer (tensor) to the nodes hosting the subsequent block(s). Note that a node may be allocated zero, one, or multiple exits, which are all executed.

We represent the overall system by means of a directed *two-dimensional load-resource, two-plane graph* model [18]–[20], with one plane capturing the network nodes and the other the blocks of the DNN layers. We establish a relationship between these two planes to represent the possible mapping between the communication and compute resource demand of the applications in $\mathcal{H}$ onto the resources made available by the multi-tiered network nodes in $\mathcal{N}$. Also, the two-dimensional load-resource model matches the communication and computing resources handled by the system, i.e., offered by the network nodes and required by the applications.

More formally, we denote such graph, illustrated in the left panel of Fig. 2, with $\widetilde{\mathcal{G}} = \{\widetilde{\mathcal{V}}, \widetilde{\mathcal{E}}\}$ where $\widetilde{\mathcal{V}}$ are the vertices and $\widetilde{\mathcal{E}}$ are the edges. The two graph planes are as follows (the notation is summarized in Table I).

Plane 1: The vertices $\widetilde{\mathcal{V}}_1 \subset \widetilde{\mathcal{V}}$ of this plane correspond to the system nodes in $\mathcal{S} \cup \mathcal{N}$. A slicing setting is in place, where applications and nodes are assigned separate portions of computing resources and bandwidth. Thus, we associate with the edges $\widetilde{\mathcal{E}}_1 \subset \widetilde{\mathcal{E}}$ bidimensional weights $[b^h(n_1, n_2), c^h(n_1, n_2)]$, $n_1, n_2 \in \mathcal{N}$, where $b^h(n_1, n_2)$ corresponds to the bandwidth of the communication link between nodes n_1 and n_2 allocated to application h, and $c^h(n_1, n_2)$ is the computing power of n_1 allocated to application h. The existence of the edge determines whether or not two nodes can communicate, and the self loop $n \to n$ has infinite capacity, i.e., $b^h(n, n) = \infty$. Further, the edge between a network node $n \in \mathcal{N}$ and a co-located data source $s \in \mathcal{S}$ has weight $[b^h(s, n), c^h(s, n)] = [\infty, 0]$, i.e., we consider the bandwidth between the two s and n as unlimited and that the data source does not have any compute capability.

Plane 2: The vertices $\widetilde{\mathcal{V}}_2 \subset \widetilde{\mathcal{V}}$ of this plane correspond to DNN layers' blocks $\mathcal{L} = \{\mathcal{L}^h\}_h$. The edges $\widetilde{\mathcal{E}}_2$ in this plane capture the connectivity structure of the DNNs, where edges exist only between consecutive blocks of the same application. The weights $[d^h(\ell_1^h, \ell_2^h), o^h(\ell_1^h, \ell_2^h)]$, $\ell_1^h, \ell_2^h \in \mathcal{L}^h$, represent the size (in bits) of the data output by block ℓ_1^h ($d^h(\ell_1^h, \ell_2^h)$) and the number of operations needed to execute block ℓ_1^h ($o^h(\ell_1^h, \ell_2^h)$).

Inter-plane edges: A set of edges $\widetilde{\mathcal{E}}_{\ell \to n}$ unidirectionally connects Plane 2 to Plane 1, with the generic edge representing that a layers' block of a DNN is deployed at a network node.

B. From the two-plane to the single-plane extended graph

We now transform the two-dimensional load-resource, two-plane graph $\widetilde{\mathcal{G}}$ into a directed *single-plane* extended graph $\mathcal{G} = \{\mathcal{V}, \mathcal{E}\}$ (second panel of Fig. 2). The vertices of $\mathcal{G}$ correspond to joint nodes and DNN blocks that are connected by inter-plane edges in $\widetilde{\mathcal{G}}$, that is, in $\mathcal{G}$ the two planes are collapsed following the connecting edges. Furthermore, an edge in $\mathcal{G}$ exists only if the corresponding nodes and DNN blocks are connected in $\widetilde{\mathcal{G}}$. Consider the vertices $v = (n, \ell_i^h)$ and $v' = (n', \ell_j^h)$, where $n, n' \in \mathcal{N}$ are network nodes and $\ell_i^h, \ell_j^h \in \mathcal{L}^h$ are DNN blocks. Notably, vertices corresponding to data sources in $\mathcal{G}$ are not bound with any DNN block.

In $\mathcal{G}$, edges exist only between nodes embedding consecutive blocks of the same DNN (which may deployed also on the same node), and are associated with the set of weights $[T^h(v, v'), C^h(v, v'), E^h(v, v')]$, where $T^h(v, v')$ and $C^h(v, v')$ are the data transfer time and the computing time, respectively, and $E^h(v, v')$ is the per-inference energy consumption. We then define $T^h(v, v')$ and $C^h(v, v')$ as:

$$T^h(v, v') = \frac{d^h(\ell_i^h, \ell_j^h)}{b^h(n, n')}, \quad C^h(v, v') = \frac{o^h(\ell_i^h, \ell_j^h)}{c^h(n, n')}. \tag{1}$$

We recall that $b^h(n, n') = \infty$ if $n = n'$, that is, the communication time is equal to 0 if the vertices are associated with different (and necessarily contiguous) DNN blocks allocated on the same node. The weight $E^h(v, v')$ instead compounds the computing, transmission, and receiving energy associated with edge $v \to v'$, i.e.,

$$E^h(v, v') = (\xi_t + \xi_r) \frac{d^h(\ell_i^h, \ell_j^h)}{b^h(n, n')} + \xi_c \frac{o^h(\ell_i^h, \ell_j^h)}{c^h(n, n')}, \tag{2}$$

where ξ_t, ξ_r and ξ_c are the power consumption spent, respectively, by node n to transmit, and by node n' to receive and compute, a data unit.

C. Energy-efficient inference: Problem formulation

First, given application h, we denote with π^h the generic configuration indicating (i) the sources feeding data to the application as well as (ii) *which* DNN blocks with early exits should be deployed (hence used) for inference, and (iii) *where* (i.e., on which network nodes). We then define binary selection variables $p_\pi^h(v) \in \{0, 1\}$ based on the configuration π^h, where $v \in \mathcal{V}$. If $p_\pi^h(v) = 1$, then the vertex v is selected by the configuration π^h, i.e., $v \in \pi^h$; if $p_\pi^h(v) = 0$, v is not selected, i.e., $v \notin \pi^h$. The configuration π^h is controlled by the orchestrator. Note that the configuration needs to build a path from the sources to the DNN output for all the applications. Further, we remark that a node may be allocated multiple blocks, and even multiple exits. In the graph representation, this corresponds to a configuration that selects multiple vertices representing the same node and separate DNN blocks (like the red path in Fig. 2(center)).

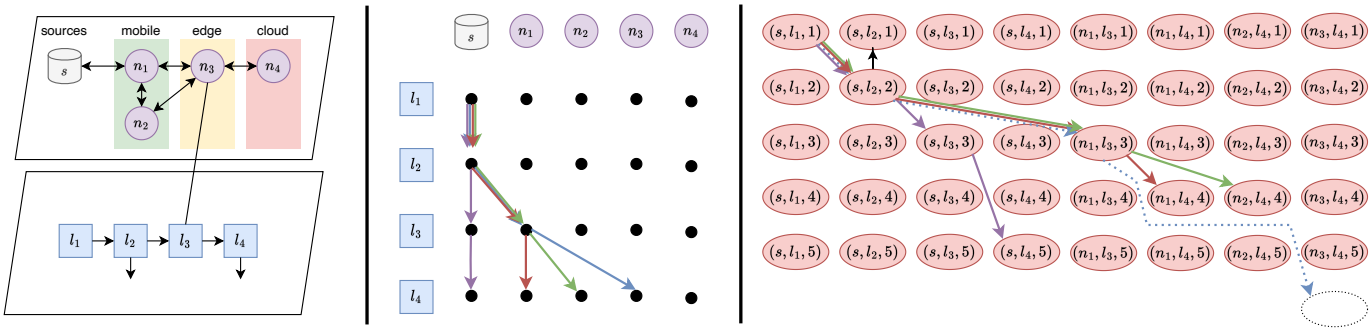

Fig. 2. The graphs used in our solution strategy: two-dimensional, two-plane system model (left); single-plane extended graph (center); feasible graph (right).

We adopt here a performance metric that is a function of the configuration and cannot be decoupled as a per-edge measure: the configuration inference quality. In fact, the configuration may suppress the execution of the blocks/exits after a certain index, for instance due to latency constraints. We thus define the inference quality of application h given configuration π^h as the quality associated with the whole sequence of DNN blocks in π^h, and denote it with $a(\pi^h)$.

The objective of the orchestrator is to minimize the overall energy consumption to support σ^h (tasks per second) inferences per second (3a), subject to latency, quality, network resource, and compute-resource constraints (3b)–(3e). Recalling that $v{=}(n,\ell_i^h)$ and $v'{=}(n',\ell_j^h)$, and $\phi^h(\ell_i^h)$ is the fraction of input samples output by ℓ_i^h, the resulting optimization problem (specified here for application h) is:

$$\min_{\pi^h} \sum_{v,v'\in\mathcal{V}} \sigma^h \phi^h(\ell_i^h) E^h(v,v') p_\pi^h(v) p_\pi^h(v') \tag{3a}$$

$$\text{s.t.} \sum_{v,v'\in\mathcal{V}} \left(T^h(v,v') + C^h(v,v')\right) p_\pi^h(v) p_\pi^h(v') \leq \delta^h \tag{3b}$$

$$a(\pi^h) \geq \alpha^h \tag{3c}$$

$$\sigma^h \phi^h(\ell_i^h) o^h(\ell_i^h,\ell_j^h) \leq c^h(v,v'), \quad \forall v,v' \in \pi^h \tag{3d}$$

$$\sigma^h \phi^h(\ell_i^h) d^h(\ell_i^h,\ell_j^h) \leq b^h(v,v'), \quad \forall v,v' \in \pi^h\,. \tag{3e}$$

Problem complexity. The above problem is very complex to solve, owing to its combinatorial nature and to the overwhelming number of existing solutions. Specifically, we prove that the problem is NP-hard.

Property 1: The problem of optimizing (3a) subject to constraints (3b)–(3e) is NP-hard.

Proof: To prove NP-hardness, we perform a reduction from a known NP-hard problem to the one under study. In particular, we show that any instance of the Steiner tree problem (STP) [21] can be transformed into a *simplified* instance of the problem introduced above. The STP is a generalization of the minimum spanning tree problem: given a weighted, undirected graph and a subset of nodes therein, the goal is to select the minimum-weight tree connecting all nodes in the subset. Given an instance of the STP, we build an instance of the problem in (3a)–(3e) by creating: (i) a data source for all the vertices to connect except one, and imposing that all such sources must be used for inference; (ii) one DNN layer, corresponding to the remaining vertex to connect; (iii) physical nodes for all intermediate vertices in the STP instance; (iv) only one of the physical nodes has enough capabilities to run the DNN layer. Also, the connectivity between nodes and data sources reproduces that of the STP instance, and one component of the weights in our problem instance is set to match the weights in the STP instance while all others are set to zero.

Solving our problem to optimality also yields an optimal solution to the STP instance, hence, the two problems are equivalent. Since the reduction takes polynomial (linear) time (each edge and vertex of the STP instance is processed once) and the STP problem is NP-hard [21], the thesis is proved. ■

It is also worth remarking that the instance of our problem created in the proof above is very simple (only one DNN layer, only one non-zero weight for the edges, etc.). This suggests that, on top of being NP-hard, our problem is significantly *more* complex than an already NP-hard problem like the STP. In light of the problem complexity, we propose below an algorithmic solution, leveraging a graph representation that, efficiently and very conveniently, embeds all possible decisions, the application requirements, and the system constraints.

III. The FIN Solution

Here, we introduce our proposed heuristic, called Feasible Inference Graph (FIN). We first describe how to build a *feasible* graph – i.e., a graph summarizing all feasible solutions to the energy-aware inference problem – starting from the extended one we used to formulate the optimization problem. By construction, the feasible graph includes only those decisions (i.e., which data sources and DNN blocks are used and where such blocks should be deployed) that meet all constraints on inference latency and quality as well as on data, computational, and network resources. The second part of the section then describes how the most energy-efficient DNN configuration can be found by identifying the minimum-cost path traversing the feasible graph, as the edge weights represent the energy consumption (computation and communication) incurred by the nodes.

Specifically, the feasible graph built by FIN summarizes all feasible solutions through two complementary strategies:

- the *additive* constraint, namely, the inference latency, is guaranteed by the graph topology itself;

- the other constraints related to system capability and application requirements, e.g., inference quality and data requirements as well as bandwidth limits, are guaranteed by pruning the edges and vertices that would violate them.

The vertices of the feasible graph are then the same as in the extended one, but each vertex is replicated a number γ of times. Let us denote the g-th replica of a vertex $v{=}(n, l_i^h){\in}\mathcal{G}$ with v_g, $g{=}1, \ldots, \gamma$, and define index g as *depth* of a vertex. The vertices depth is what allows us to track the additive constraints – in our case, inference latency. Indeed, different replicas v_g of the same vertex v correspond to situations that are equivalent *except for the accumulated inference latency*: intuitively, the deeper a vertex, the closer it is to violating the additive constraint on the inference latency. Importantly, as mentioned earlier, all vertices correspond to solutions that do honor the latency limit; for vertices whose depth is exactly γ the constraint (3b) is met with an equality sign.

Once the vertices are in place, we proceed to creating the edges connecting them. Specifically, we create an edge from vertex v_{g_1} to vertex v'_{g_2}, with $v'{=}(n', l_j^h)$ and $g_2{>}g_1$, if:

- it is possible to place layer ℓ_i^h at node n and layer ℓ_j^h at node n';
- doing so incurs a combined processing time and network delay such that:

$$g_2 - g_1 = \left\lceil \gamma \cdot \frac{T^h(v, v') + C^h(v, v')}{\delta^h} \right\rceil . \tag{4}$$

In the numerator of the fraction above, the first term corresponds to the computing time, and the second to the data transfer delay.

Let us then define the steepness of an edge as the difference between the depth of the target and the source vertices, and the steepness of a path as the sum of the steepness values of its edges. Intuitively, steeper edges (and steeper paths) correspond to solutions with a longer inference latency; also, any path arriving to a vertex corresponding to an exit layer before depth γ represents, by construction, a solution conforming with the latency limit constraint.

Next, we prune all the vertices and edges that do not conform with the *local* constraints, i.e.,

- edges that would not reach the target inference quality, i.e., they belong to a configuration π^h s.t. $a(\pi^h){<}\alpha^h$, or
- edges that would exceed the available bandwidth or computational capability of the node represented by the vertex tail of the edge, i.e., $\sigma^h \phi^h(\ell_i^h) d^h(\ell_i^h, \ell_j^h) {>} b^h(v, v')$ or $\sigma^h \phi^h(\ell_i^h) o^h(\ell_i^h, \ell_j^h) {>} c^h(v, v')$.

Surviving edges are assigned a weight corresponding to the energy consumption they incur, as defined in (2). Thanks to the way the feasible graph is built and pruned, any path going from a data source vertex to any vertex corresponding to an exit layer corresponds to a feasible solution. To find the optimal one, it is thus sufficient to compute the minimum-cost path.

For instance, the right panel of Fig. 2 depicts a feasible graph with $\gamma{=}5$. The red and green paths have steepness 3 and the purple one has steepness 4; they are all feasible and one of them will be selected as optimal solution. The blue path, instead, *would* have a steepness of 5 and terminate at node $(n_4, l_4, 6)$; but this node does not exist in the feasible graph. The blue path as a whole is thus infeasible (hence, it is dotted in the figure), and is dropped from the graph.

As for parameter γ, this indicates the *resolution* with which the inference latency is represented by the feasible graph: the smaller the γ values, the fewer the quantization levels (hence, the possible values of vertex depth and path steepness), and the larger the quantization error. As shown in Property 2, such an error can be arbitrarily reduced by increasing γ, thus getting arbitrarily close to the optimum.

Property 2: The competitive ratio of FIN (i.e., the ratio of the cost of FIN's solution to the cost of the optimal one) is $1{+}\frac{1}{\gamma}$.

Proof: FIN consists of two steps: (a) building the feasible graph and (b) finding a minimum-cost path on it. Step (b) can be solved to optimality, e.g., through the Bellman-Ford algorithm. Step (a) can use the result of [22, Th. 4.3], proving that creating γ replicas of the vertices in the feasible graph results in a cost increase of at most $\frac{1}{\gamma}$ times the optimum. ■

On the negative side, a high value of γ results in a higher complexity as the minimum-cost traversal will search for more edges in the feasible graph. It is thus essential to set a value of γ that effectively trades off quantization error with complexity. Furthermore, given γ, we envision a λ-proximity approach to reduce the complexity in searching for the vertices and edges to include in the output configuration. Specifically, as the vertices with small depth have a lower number of outgoing feasible edges, searching among vertices with depth close to 1 may not help. We thus limit the search to a λ-proximity ($1{\leq}\lambda{\leq}\gamma$) index on the maximum depth vertices, i.e., with index $g{\in}[(\gamma{-}\lambda), \gamma]$, and $\lambda{=}\gamma$ corresponding to the exhaustive search among all nodes.

The steps involved in FIN are described in Alg. 1 and depicted in Fig. 3; the figure also shows how FIN is integrated with the construction of the two-plane system graph and the single-plane extended graph.

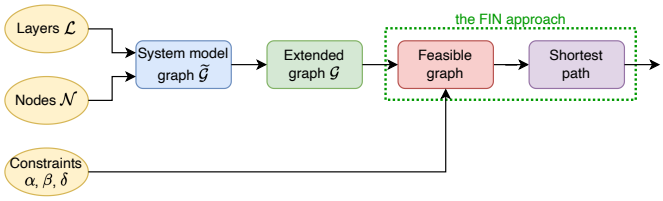

Fig. 3. Solution strategy and steps within FIN.

IV. Reference Scenario

Branched DNNs with early-exits. To evaluate the performance of our FIN solution, we consider six different applications corresponding to three DNN models with early-exits, namely, B-LeNet, B-AlexNet, and B-ResNet, each trained with two popular datasets. We summarize such mapping in Table II and detail the three models below. We also underline that we consider accuracy as measure of the inference quality.

Algorithm 1: FIN: Feasible graph and configuration selection

Input: $\mathcal{G}$, α^h, δ^h, γ, λ

Function I: Create_feasible_graph ($\mathcal{G}$,γ) **:**

1) **Create replica vertices**

for *each vertex* $v \in \mathcal{V}$ **do**

for $g = 0 : 1 : \gamma$ **do**

Create v_g and include in feasible vertex set

2) **Create directed edges**

for *each edge* $(v, v') \in \mathcal{E}$ **do**

for $g_1 = 0 : 1 : \gamma$ **do**

for $g_2 = i : 1 : \gamma$ **do**

if (4) *holds true* **then**

Create edge (v_{g_1}, v'_{g_2});

Include it in feasible edges set;

Compute edge weight $E_h(v_{g_1}, v'_{g_2})$ using (2);

return feasible graph

Function II: Configuration_solution (*feasible graph,* λ, γ) **:**

1) Minimum-cost path traversal on feasible graph, over λ-proximity vertices (i.e., v_g with $g \in [(\gamma - \lambda), \gamma]$)

Initialize $g_1 = 1$

Include $v_{g_1} = (n, l_1^h)$ in π^h

for $i = 2 : |\mathcal{L}^h|$ **do**

for $g_2 = (\gamma - \lambda) : \gamma$ **do**

if *edge* (v_{g_1}, v'_{g_2}): $v_{g_1} = (n, l_{i-1}^h)$ **then**

Include v'_{g_2} in π^h if $\min_{v'} E^h(v, v')$;

Set $g_1 = g_2$;

return π^h as FIN output configuration

TABLE II
DETAILS OF THE PRE-TRAINED DNN MODELS WITH EARLY EXITS USED BY THE SIX APPLICATIONS

Application	DNN	Training dataset	# exits	Exit output ϕ^h [%]
h_1	B-AlexNet	CIFAR100	3	[65.6, 25.2, 9.2]
h_2		CIFAR10	3	
h_3	B-ResNet	CIFAR100	3	[41.5, 13.8, 44.7]
h_4		CIFAR10	3	
h_5	B-LeNet	MNIST	2	[94.3, 5.63]
h_6		EMNIST	2	

B-AlexNet is a branchy version of AlexNet [23] DNN architecture with early-exits. It has 5 convolution, 1 max-pooling, 3 fully connected, and 3 early-exit blocks. It can be used for image classification [23], video summarization [24], and human activity classification [14], [25]–[27]. The input to the B-AlexNet model is RGB format images, scaled to size 227×227×3. The feature map and complexity of the B-AlexNet architecture is given in Table III; when trained with datasets from different sources and with different sample rate (i.e., samples/category in CIFAR10 and CIFAR100) [15], it results in an accuracy level as given in Table IV.

B-ResNet is a branchy version of ResNet110 [28] DNN with early-exits used for image recognition and classification tasks. ResNet110 consists of 3 stages, with each stage comprising a series of residual blocks. The first stage has 18 residual blocks with 16 filters in each block, while the second and third stages have 36 residual blocks, each with 32 and 64 filters in each block (resp.). The residual blocks consist of 2 or 3 convolutional layers, each followed by batch normalization and ReLU activation. The input is size 32×32×3, while the feature map and complexity of B-ResNet architecture layers are given in Table III. The inference accuracy of pretrained B-ResNet using CIFAR10 and CIFAR100 is given in Table IV.

TABLE III
NUMBER OF INPUT FEATURES AND COMPLEXITY OF THE DNN MODEL BLOCKS

Block	[Number of features, Complexity [MOPs]]		
	B-AlexNet	B-ResNet	B-LeNet
1	[290400, 0.043]	[16384, 0.004]	[4704, 0.118]
2	[186624, 6.711]	[16384, 0.021]	[1600, 0.040]
3	[64896, 10.145]	[16384, 0.021]	[120, 0.048]
4	[64896, 13.523]	[4096, 0.083]	-
5	[43264, 29.045]	[4096, 0.664]	-
Exit-1	[64896, 22.579]	[4096, 0.748]	[120, 0.05]
Exit-2	[43264,9.056]	[4096, 0.665]	[10, 0.022]
Exit-3	[1000, 0.039]	[10, 0.001]	-

TABLE IV
INFERENCE ACCURACY OF THE PRE-TRAINED DNN MODELS WITH EARLY EXITS USED BY THE APPLICATIONS

Exit block	Accuracy [%]					
	h_1	h_2	h_3	h_4	h_5	h_6
Exit-1	39.56	56.37	29.97	38.97	91.18	93.54
Exit-2	54.22	78.04	39.93	51.93	96.70	99.20
Exit-3	60.32	85.95	72.21	93.91	-	-

TABLE V
COMMUNICATION (DOWNLINK (DL)/UPLINK (UL)) CAPACITY AND ENERGY CONSUMPTION OF THE SYSTEM NODES

Node	Power [W]		Traffic DL/UL [Gbps]	Energy DL/UL [nJ/bit]
	Idle	Max		
Mobile	3.1	3.7	0.1	30
Edge	4,096	4,550	560	37
Cloud	11,070	12,300	4,480	12.6

B-LeNet is a branchy version of LeNet-5 CNN architecture [29] that can recognize handwritten digits using datasets like MNIST [30] and EMNIST [31]. B-Lenet consists of 8 layers (2 convolutional, 2 subsampling, 3 fully-connected, 1 early-exit). Its feature map and complexity are given in Table III, while the inference accuracy of pretrained B-Lenet using MNIST [30] and EMNIST [31] is given in Table IV.

Network system. We use three types of nodes, i.e., mobile, edge, and cloud nodes [32], respectively, associated with the following values of computational capability in trillions operations per second (TOPS) and power consumption in watt (W): [11 TOPS, 6 W]; [153.4 TOPS, 140 W], [312 TOPS, 400 W]. The capability of the communication interface of such nodes are given in Table V [33]–[35]. We recall that such parameters define the bandwidth and computing resource weights of the edges between the vertices in Plane 1 of graph $\widetilde{\mathcal{G}}$, and the corresponding power consumption. Further, in our experiments, we initially consider one node for each network tier, and then we let the number of mobile nodes increase with the number of users.

V. Performance Evaluation

In this section, we first show the impact of different DNN configurations on the inference latency, quality, and energy cost. Then, we introduce the alternatives against which we compare FIN, and present the performance obtained for the applications and network system described earlier.

A. Impact of the DNN configurations

We start by investigating the trade-off among energy consumption, inference accuracy, and inference latency while dynamically orchestrating a DNN model on the multi-tiered network for various user applications. To this end, we consider three example configurations for B-AlexNet and B-ResNet, in which the DNN blocks are deployed on the mobile, edge, and cloud nodes as indicated in Table VI.

Fig. 4 shows that, as expected, both Config-2 (involving mobile and edge) and Config-3 (involving all tiers) reduce the inference latency overall compared to Config-1 (involving the mobile only). However, it is interesting to observe that the benefit of involving the cloud in the inference task (i.e., Config-3) is negligible when compared to Config-2 where only the edge is added in support to the mobile node.

Looking instead at the energy consumption and the accuracy performance together, while Config-2 and Config-3 make the computing burden at the mobile nodes lighter, they may imply a higher overall cost due to the communication energy expenditure. Such an expenditure appears whenever exit-2 and exit-3 are enabled (i.e., a higher accuracy is required). The increase in communication energy is especially noticeable for B-AlexNet, which has indeed the largest size, resulting in a significant surge (87.6%) in the overall cost when transitioning from Config-1 to Config-2, and a further increase of 28% when shifting from Config-2 to Config-3. Instead, whenever a lower accuracy is acceptable, we can exploit the splits corresponding to exit-1 for all DNNs, and, so doing, reduce both inference latency (from 6.56 ms to 2.67 ms), and energy consumption (from 39.4 mJ with all three exits active to just 16.4 mJ when only exit-1 is activated in Config-1).

In summary, whenever the mobile nodes are used, even for a subset of the DNN blocks, the inference latency grows to such an extent that the reduction in computing time brought by cloud nodes is negligible. Furthermore, whenever we aim at the maximum accuracy, using cloud nodes may lead to very high communication energy costs. Remarkably, however, there exist configurations involving nodes from the different network tiers that can reduce the total as well as the mobile node energy expenditure. It follows that it is possible to identify DNN allocation strategies that improve the sustainability of inference tasks when the application requirements warrant it.

TABLE VI
Example test deployment configurations of B-AlexNet and B-ResNet

Configuration		Mobile	Edge	Cloud
B-AlexNet B-ResNet	Config-1	All blocks	-	-
	Config-2	ℓ_1^h,exit-1,ℓ_2^h,	ℓ_3^h,exit-2,ℓ_4^h, ℓ_5^h,exit-3	-
	Config-3	ℓ_1^h,exit-1,ℓ_2^h,	ℓ_3^h,exit-2,ℓ_4^h	ℓ_5^h,exit-3

B. FIN performance

Benchmarks. We compare FIN against:

- *Multi-constrained path selection (MCP)*, a solution to our problem based on the multi-constrained path selection in [17]. We select [17] because no scheme exists that specifically tackles the problem at hand. [17] finds a path between source and destination nodes in a graph such that it satisfies the multiple end-to-end constraints on the additive edge weights. MCP applies such an approach to our extended graph $\mathcal{G}$ to find a feasible solution for the optimization problem in Sec. II-C. To this end, we assign to edge $v \to v' \in \mathcal{E}$ the auxiliary weight: $\Omega(v,v') = (\frac{T^h(v,v') + C^h(v,v')}{\delta^h} + \frac{a(v')}{\alpha^h})$, where $a(v')$ is the accuracy associated with the whole sequence of DNN blocks till v'. Then, the minimum-cost path is selected using the auxiliary edge weights in the extended graph.
- *Optimum (Opt),* obtained through exhaustive search.

Performance of DNN deployments. The total energy consumption of the B-AlexNet deployment configurations obtained using MCP, FIN, and Opt is presented in Fig. 5, as the inference accuracy and latency constraints vary. The corresponding breakdown into communication and computation energy consumption is depicted instead in Fig. 6. Fig. 5 shows that the energy consumption of the DNN configurations yielded by FIN (γ=10) is very close to the optimum and much less than MCP, while meeting the accuracy target α^h=80% and the latency target δ^h=5 ms. Also, for an extremely low value of γ (namely, 3), FIN still outperforms MCP. Our experiments have also revealed that such performance (α^h=80%, δ^h=5 ms) is achieved by MCP, FIN (γ=10), and Opt deploying (resp.) a set of [3,1,1], [2,1,2], and [1,2,2] blocks on

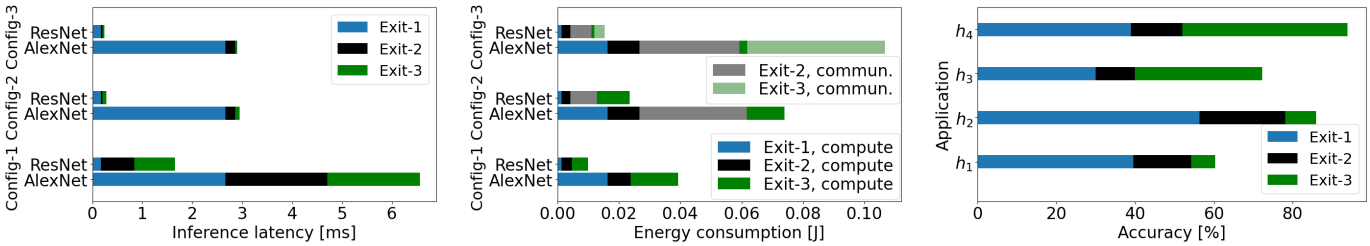

Fig. 4. Impact of the configurations listed in Table VI: inference latency (left) and energy consumption (center) for the B-AlexNet and B-ResNet; inference accuracy for B-AlexNet-based h_1, h_2 and B-ResNet-based h_3, h_4 (right).

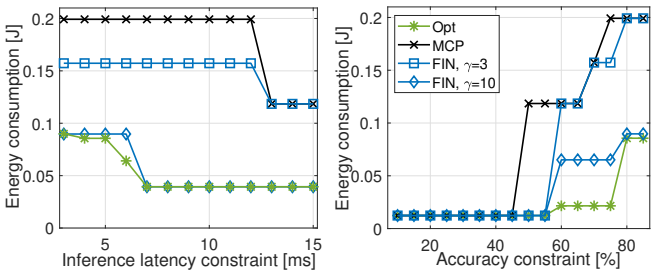

(a) α^h =80% (b) δ^h =5 ms

Fig. 5. Total energy consumption of the B-AlexNet configurations obtained through Opt, MCP, and FIN (γ=3, 10), as the target inference latency and accuracy vary.

[mobile, edge, cloud] nodes, and each employs exit-3 to meet the target accuracy. In this case, the deployment of the last two DNN blocks on the cloud reduces the energy consumption in FIN and Opt configuration as compared to MCP. For a less stringent latency requirement (α^h=80%, δ^h=12 ms), MCP deploys [1,4,0] while FIN (γ=10) and Opt both deploy [5,0,0] blocks, as the larger target latency allows keeping all blocks on the mobile, which reduces energy consumption. In summary, meeting a smaller inference latency target requires a split deployment that increases energy expenditure.

TABLE VII
EXECUTION-TIME [MS] TAKEN BY MCP AND FIN (γ = 3, 10) FOR FINDING THE DEPLOYMENT CONFIGURATION OF EACH DNN

Model	MCP	FIN	
		γ=3	γ=10
B-AlexNet	0.591	0.892	2.450
B-ResNet	0.545	0.657	1.158
B-LeNet	0.243	0.461	0.816

This is confirmed by Fig. 6(a)(c): for a lower target inference latency, communication energy consumption grows, as a split deployment is needed. Similarly, Fig. 6(b)(d) underline that, with a higher value of accuracy constraint, the best configurations incur higher computation and communication energy:

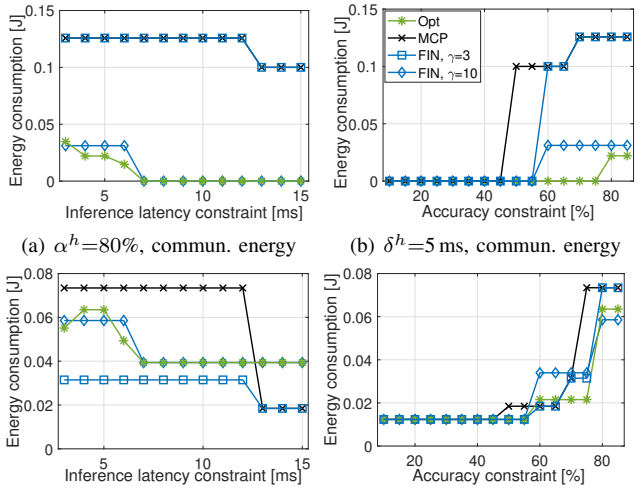

(a) α^h=80%, commun. energy (b) δ^h=5 ms, commun. energy

(c) α^h=80%, compute energy (d) δ^h=5 ms, compute energy

Fig. 6. Computation and communication energy consumption of MCP, FIN, Opt for B-AlexNet configurations, as the constraints vary.

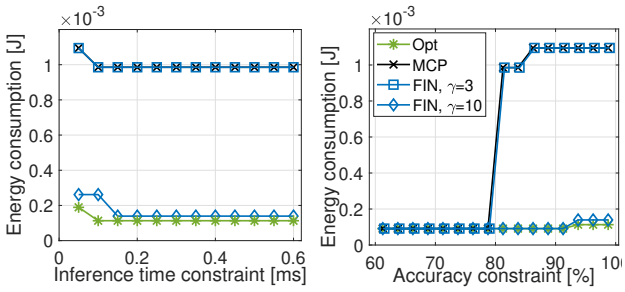

(a) α^h=85 % (b) δ^h=0.1 ms

Fig. 7. Total energy consumption of the B-LeNet configurations obtained through Opt, MCP, and FIN (γ=3, 10), as the target inference latency and accuracy vary.

indeed, inspecting the resulting deployments, it emerges that they require later exit (exit-3) and split deployment. Comparing FIN to its benchmarks, two main aspects are evident. First, even for a moderate value of γ=10, FIN virtually always matches the optimum and significantly outperforms MCP in all cases. When γ drops to 3, the communication and computation energy expenditures diverge: the former (Fig. 6(a)(b)) deteriorates significantly; the latter (Fig. 6(c)(d)) remains remarkably low and stays close to the optimum. This suggests that communication energy is *harder* to minimize than computation energy, owing to the complexity of the scenarios we target. Importantly, even when γ=3 – which, it is worth remarking, is extremely low – FIN can match MCP. We have similarly evaluated the B-ResNet (omitted for brevity) and the B-LeNet deployments (Fig. 7). Looking at FIN's energy consumption, a similar effect to Fig. 5 emerges, with FIN now matching the optimum for sufficiently high γ even more closely than in the case of B-AlexNet.

Table VII lists the overall execution times taken (on average) by MCP and FIN (γ=3, 10) for obtaining the deployment configuration of the B-AlexNet, B-ResNet, and B-LeNet models, using a Lenovo ThinkPad P1 Gen 3 with i7-10750H CPU (2.6 GHz, 32 GB RAM). The execution time of FIN is shorter than twice that of MCP for γ=3 and shorter than 5 times for γ=10. Overall, the execution time of FIN is less than 2.5 ms.

Multi-application scenario. We now apply FIN to the deployment of the six applications listed in Table II. Using the pre-trained DNN models for inference, we investigate the impact of an increasing number of users on the system performance. We consider that 0.5% of the edge and cloud computing resources are available for each of the applications' inference execution. The application requirements, [inference latency [ms], accuracy [%]], are set to [5,55], [5, 55], and [0.1, 93] for h_{1-2}, h_{3-4}, and h_{5-6} applications, respectively. The energy consumption (computing and communication) gain provided by FIN (γ=10) and MCP, for the running applications h_{1-6} that require one-inference-per-second-per-user, is shown in Fig. 8 (the size of this scenario renders obtaining the optimum impractical). Notice how FIN deploys the DNN model configuration that entails an overall energy consumption that is 65%–70% of the benchmark for all the considered DNNs (Fig. 8(left)). Also, the MCP approach leans

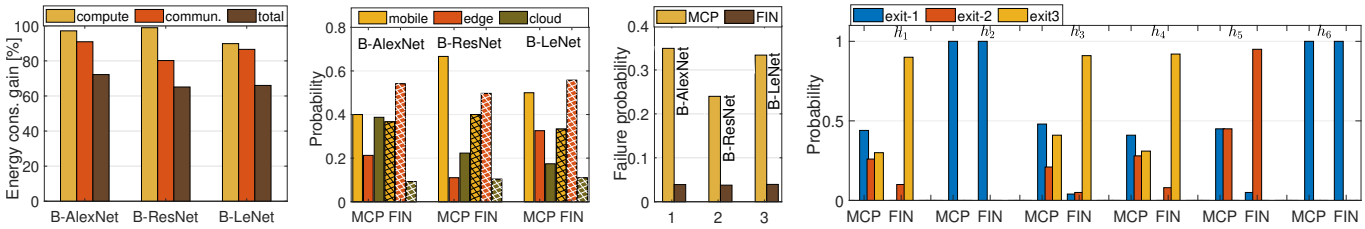

Fig. 8. Performance in the multi-application scenario: Energy consumption gain through FIN over MCP (left); probability of DNN block deployment on the multi-tier nodes in MCP and FIN (center-left), that the selected configuration fails to meet the constraints (center-right), and of DNN exit point for inference (right). For FIN, we set γ=10.

towards more deployment on the mobile and cloud side, whereas FIN takes full advantage of all tiers and, in particular, of the edge (Fig. 8(center-left)). Not only does FIN achieve better energy efficiency, but it also surpasses MCP in terms of success probability across all applications (Fig. 8(center-right)). In contrast to MCP's high failure probability (over 30% for B-Alexnet and B-Lenet and 20% for B-Resnet), FIN sees less than 5% of users failing to meet the latency and accuracy constraints. Consistently, Fig. 8(right) shows that, with high probability and unlike MCP, FIN can deploy the applications blocks all the way to exit-3 whenever required, while it rightfully enables the earliest exit split whenever the accuracy constraint allows it (e.g., for h_2 and h_6).

VI. Related Work

Our work lies at the intersection of two major fields, namely, model split (or, partitioning) and resource-aware ML.

Early exit and model splitting [8]: Early exit models have been introduced in [14], which also raises the issue of how to place the early-exit layers, i.e., how to make the DNN topology *branchy*. In the same context, [9] tackles distributed scenarios and seeks to adapt the placement of exit layers to the available resources in the near-edge, edge, and cloud segments of the network. [10] pursues a similar approach in IoT scenarios, minimizing the usage of edge resources. More recent work [12] performs DNN splitting in real time, with the aim of adapting to changes in channel conditions. The recent work [13] widens the focus and accounts for the location of the users that need the inference task.

Earlier approaches seek to split DNNs at naturally-occurring suitable locations, a.k.a. *bottlenecks* [36], [37]. If no bottleneck is available, the related problem of *bottleneck injection* arises. The goal is to change the topology of the DNN with the aim of creating suitable points to insert an early-exit layer. These techniques have been pioneered by [38], [39], and often use pairs of encoder and decode layers. Bottleneck injection can be performed in a content-aware fashion, as in [40], [41]. Also, [5] underlines that collaborative DNN partitioning and task offloading in resource-constrained edge-IoT network can meet the DNN inference deadline requirements.

Resource-aware ML is, broadly speaking, concerned with adapting the distributed ML task to perform (whether it is training or inference) and the available resources. Works in this field often focus on selecting the best nodes to exploit, accounting for their speed [42], size of local dataset [43], and feature-richness thereof [44], as well as any communication issues they may experience [45]. A more recent trend, closer in spirit to model partitioning, consists in changing the learning task to fit the available resources, e.g., by selecting the most appropriate model [46].

A related trend is reliability in distributed ML. The main goal of this line of work is ensuring that all nodes involved in the ML task provide timely and high-quality updates, despite communication issues [47] and the presence of malicious nodes [48]. Reliability might be at odd with fairness issues, and a balance between the two goals is sought in [49].

In summary, to the best of our knowledge, our work is the first to jointly tackle (i) how ML model splitting should be performed and (ii) where the different model blocks should be deployed, (iii) for models with early exits as well as in the presence of inference requirements and constraints on the computational and networking resources in multi-tier systems.

VII. Conclusions

This paper addresses the problem of allocating sections of multi-branched dynamic DNNs to nodes in mobile-edge-cloud systems. By means of a multi-stage graph-modeling approach, we solve the problem of minimizing the inference energy cost while matching the inference target requirements to the constrained nodes' resources. Our algorithmic solution, named FIN, to this (NP-hard) problem leverages a further manipulation of the graph model to yield a low-complexity, yet effective, solution strategy. The results show that FIN closely matches the optimum and, by enabling effective split deployments and leveraging at best the nodes of the multi-tiered network, reduces by over 65% the inference energy consumption with respect to our benchmark. Future work will optimize the allocation of bandwidth and computational resources across different DNN-based applications in a multi-tier system.

Acknowledgments

This work was supported by the European Commission through Grant No. 101095890 (PREDICT-6G project), Grant No. 101096379 (CENTRIC project), and Grant No. 101095363 (ADROIT6G project), and by the European Union under the Italian National Recovery and Resilience Plan (NRRP) of NextGenerationEU, partnership on "Telecommunications of the Future" (PE0000001 - program "RESTART").

REFERENCES

[1] Z. Li, F. Liu, W. Yang, S. Peng, and J. Zhou, "A survey of convolutional neural networks: analysis, applications, and prospects," *IEEE transactions on neural networks and learning systems*, 2021.

[2] A. B. Nassif, I. Shahin, I. Attili, M. Azzeh, and K. Shaalan, "Speech recognition using deep neural networks: A systematic review," *IEEE access*, vol. 7, pp. 19 143–19 165, 2019.

[3] Y. Goldberg, *Neural network methods for natural language processing*. Springer Nature, 2022.

[4] I. Azimi, A. Anzanpour, A. M. Rahmani, T. Pahikkala, M. Levorato, P. Liljeberg, and N. Dutt, "Hich: Hierarchical fog-assisted computing architecture for healthcare iot," *ACM Transactions on Embedded Computing Systems*, 2017.

[5] X. Zhang, M. Mounesan, and S. Debroy, "EFFECT-DNN: energy-efficient edge framework for real-time DNN inference," in *Proc. IEEE WoWMoM*, Boston, MA, USA, June 2023, pp. 10–20.

[6] L. Deng, G. Li, S. Han, L. Shi, and Y. Xie, "Model compression and hardware acceleration for neural networks: A comprehensive survey," *Proceedings of the IEEE*, vol. 108, no. 4, pp. 485–532, 2020.

[7] Q. Luo, S. Hu, C. Li, G. Li, and W. Shi, "Resource scheduling in edge computing: A survey," *IEEE Communications Surveys & Tutorials*, vol. 23, no. 4, pp. 2131–2165, 2021.

[8] Y. Matsubara, M. Levorato, and F. Restuccia, "Split computing and early exiting for deep learning applications: Survey and research challenges," *ACM Computing Surveys*, vol. 55, no. 5, pp. 1–30, 2022.

[9] Y. Kang, J. Hauswald, C. Gao, A. Rovinski, T. Mudge, J. Mars, and L. Tang, "Neurosurgeon: Collaborative intelligence between the cloud and mobile edge," *ACM SIGARCH Computer Architecture News*, 2017.

[10] Y.-T. Yang and H.-Y. Wei, "Edge–iot computing and networking resource allocation for decomposable deep learning inference," *IEEE Internet of Things Journal*, vol. 10, no. 6, pp. 5178–5193, 2022.

[11] W. Miao, Z. Zeng, L. Wei, S. Li, C. Jiang, and Z. Zhang, "Adaptive dnn partition in edge computing environments," in *IEEE ICPADS*, 2020.

[12] J. Lee, H. Lee, and W. Choi, "Wireless channel adaptive dnn split inference for resource-constrained edge devices," *IEEE Communications Letters*, 2023.

[13] W. Fan, L. Gao, Y. Su, F. Wu, and Y. Liu, "Joint dnn partition and resource allocation for task offloading in edge-cloud-assisted iot environments," *IEEE Internet of Things Journal*, 2023.

[14] S. Teerapittayanon *et al.*, "Branchynet: Fast inference via early exiting from deep neural networks," in *IEEE ICPR*, 2016.

[15] R. Dong, Y. Mao, and J. Zhang, "Resource-constrained edge ai with early exit prediction," *Journal of Communications and Information Networks*, vol. 7, no. 2, pp. 122–134, Jun. 2022.

[16] S. Laskaridis, A. Kouris, and N. D. Lane, "Adaptive inference through early-exit networks: Design, challenges and directions," in *Proceedings of the 5th International Workshop on Embedded and Mobile Deep Learning*, 2021, pp. 1–6.

[17] G. Xue, A. Sen, W. Zhang, J. Tang, and K. Thulasiraman, "Finding a path subject to many additive QoS constraints," *IEEE/ACM Transactions on Networking*, vol. 15, no. 1, pp. 201–211, Feb. 2007.

[18] L. Gouveia, M. Leitner, and M. Ruthmair, "Layered graph approaches for combinatorial optimization problems," *Computers & Operations Research*, vol. 102, pp. 22–38, Feb. 2019.

[19] ——, "Extended formulations and branch-and-cut algorithms for the black-and-white traveling salesman problem," *European Journal of Operational Research*, vol. 262, no. 3, pp. 908–928, Nov. 2017.

[20] S. Yang, F. Li, S. Trajanovski, X. Chen, Y. Wang, and X. Fu, "Delay-aware virtual network function placement and routing in edge clouds," *IEEE Transactions on Mobile Computing*, 2021.

[21] F. K. Hwang *et al.*, "Steiner tree problems," *Networks*, 1992.

[22] G. Xue, A. Sen, W. Zhang, J. Tang, and K. Thulasiraman, "Finding a path subject to many additive qos constraints," *IEEE/ACM Transactions on networking*, 2007.

[23] O. Elharrouss, Y. Akbari, N. Almaadeed, and S. Al-Maadeed, "Backbones-review: Feature extraction networks for deep learning and deep reinforcement learning approaches," Jun. 2022. [Online]. Available: https://arxiv.org/abs/2206.08016

[24] J. Lei, Q. Luan, X. Song, X. Liu, D. Tao, and M. Song, "Action parsing-driven video summarization based on reinforcement learning," *IEEE Transactions on Circuits and Systems for Video Technology*, 2019.

[25] F. Serpush and M. Rezae, "Complex human action recognition using a hierarchical feature reduction and deep learning-based method," *SN Computer Science*, vol. 2, no. 94, pp. 1–15, Feb. 2021.

[26] A. Ullah, J. Ahmad, K. Muhammad, M. Sajjad, and S. W. Baik, "Action recognition in video sequences using deep bi-directional LSTM with CNN features," *IEEE Access*, vol. 6, pp. 1155–1166, 2018.

[27] S. Darafsh, S. S. Ghidary, and M. S. Zamani, "Real-time activity recognition and intention recognition using a vision-based embedded system," *CoRR*.

[28] K. He, X. Zhang, S. Ren, and J. Sun, "Deep residual learning for image recognition," 2015.

[29] Y. Lecun, L. Bottou, Y. Bengio, and P. Haffner, "Gradient-based learning applied to document recognition," *Proceedings of the IEEE*, 1998.

[30] Y. LeCun, C. Cortes, and C. Burges, "Mnist handwritten digit database," *ATT Labs*, 2010.

[31] G. Cohen, S. Afshar, J. Tapson, and A. van Schaik, "Emnist: an extension of mnist to handwritten letters," *arXiv preprint arXiv:1702.05373*, 2017.

[32] F. Malandrino, C. F. Chiasserini, and G. di Giacomo, "Efficient distributed DNNs in the mobile-edge-cloud continuum," *IEEE/ACM Transactions on Networking (early access)*, pp. 1–15, Nov. 2022.

[33] F. Jalali, K. Hinton, R. Ayre, T. Alpcan, and R. S. Tucker, "Fog computing may help to save energy in cloud computing," *IEEE Journal on Selected Areas in Communications*, 2016.

[34] Y. Li, A.-C. Orgerie, I. Rodero, B. L. Amersho, M. Parashar, and J.-M. Menaud, "End-to-end energy models for edge cloud-based IoT platforms: Application to data stream analysis in IoT," *Future Generation Computer Systems*, vol. 87, pp. 667–678, Oct. 2018.

[35] L. Sun, H. Deng, R. K. Sheshadri, W. Zheng, and D. Koutsonikolas, "Experimental evaluation of WiFi active power/energy consumption models for smartphones," *IEEE Transactions on Mobile Computing*, vol. 16, no. 1, pp. 115–129, Mar. 2017.

[36] C. Buciluǎ, R. Caruana, and A. Niculescu-Mizil, "Model compression," in *ACM SIGKDD*, 2006.

[37] C.-H. Chiang, P. Liu, D.-W. Wang, D.-Y. Hong, and J.-J. Wu, "Optimal branch location for cost-effective inference on branchynet," in *IEEE Big Data*, 2021.

[38] Y. Matsubara, S. Baidya, D. Callegaro, M. Levorato, and S. Singh, "Distilled split deep neural networks for edge-assisted real-time systems," in *ACM HotEdgeVideo*, 2019.

[39] A. E. Eshratifar, A. Esmaili, and M. Pedram, "Bottlenet: A deep learning architecture for intelligent mobile cloud computing services," in *IEEE/ACM ISLPED*, 2019.

[40] J. C. Lee, Y. Kim, S. Moon, and J. H. Ko, "A splittable dnn-based object detector for edge-cloud collaborative real-time video inference," in *IEEE AVSS*, 2021.

[41] Y. Matsubara, D. Callegaro, S. Singh, M. Levorato, and F. Restuccia, "Bottlefit: Learning compressed representations in deep neural networks for effective and efficient split computing," in *IEEE WoWMoM*, 2022.

[42] S. Wang, T. Tuor, T. Salonidis, K. K. Leung, C. Makaya, T. He, and K. Chan, "Adaptive federated learning in resource constrained edge computing systems," *IEEE Journal on Selected Areas in Communications*, 2019.

[43] F. Malandrino and C. F. Chiasserini, "Federated learning at the network edge: When not all nodes are created equal," *IEEE Communications Magazine*, 2021.

[44] H. Wu and P. Wang, "Fast-convergent federated learning with adaptive weighting," *IEEE Transactions on Cognitive Communications and Networking*, 2021.

[45] Y. Zhou, Q. Ye, and J. C. Lv, "Communication-Efficient Federated Learning with Compensated Overlap-FedAvg," *IEEE Transactions on Parallel and Distributed Systems*, 2021.

[46] F. Paissan, A. Ancilotto, A. Brutti, and E. Farella, "Scalable neural architectures for end-to-end environmental sound classification," in *IEEE ICASSP*, 2022.

[47] F. Ang, L. Chen, N. Zhao, Y. Chen, W. Wang, and F. R. Yu, "Robust federated learning with noisy communication," *IEEE Transactions on Communications*, 2020.

[48] S. Li, Y. Cheng, W. Wang, Y. Liu, and T. Chen, "Learning to detect malicious clients for robust federated learning," *arXiv preprint arXiv:2002.00211*, 2020.

[49] T. Li, S. Hu, A. Beirami, and V. Smith, "Ditto: Fair and robust federated learning through personalization," in *ICML*, 2021.